Applied Mathematics and Computation 217 (2010) 2339–2347

Contents lists available at ScienceDirect

Applied Mathematics and Computation

journal homepage: www.elsevier.com/locate/amc

The effect of boundary conditions on the mesoscopic lattice Boltzmann method: Case study of a reaction–diffusion based model for Min-protein oscillation

Waipot Ngamsaad [a], Paisan Kanthang [a], Charin Modchang [a], Somchai Sriyab [b], Wannapong Triampo [a,c,*]

[a] R&D Group of Biological and Environmental Physics, Department of Physics, Faculty of Science, Mahidol University, Bangkok 10400, Thailand
[b] Department of Mathematics, Faculty of Science, Mahidol University, Bangkok 10400, Thailand
[c] Center of Excellence for Vector and Vector-Borne Diseases, Faculty of Science, Mahidol University, Nakhon Pathom 73170, Thailand

ARTICLE INFO

Keywords:
Lattice Boltzmann method
Boundary conditions
Min-protein oscillation
Cell division

ABSTRACT

Min-protein oscillation in *Escherichia coli* has an essential role in controlling the accurate placement of the cell division septum at the middle-cell zone of the bacteria. This biochemical process has been successfully described by a set of reaction–diffusion equations at the macroscopic level. The lattice Boltzmann method (LBM) has been used to simulate Min-protein oscillation and proved to recover the correct macroscopic equations. In this present work, we studied the effects of LBM boundary conditions (BC) on Min-protein oscillation. The impact of diffusion and reaction dynamics on BCs was also investigated. It was found that the mirror-image BC is a suitable boundary treatment for this Min-protein model. The physical significance of the results is extensively discussed.

1. Introduction

Cell division is a crucial event in the life of every organism. Most bacteria divide symmetrically so that both of the newly formed daughter cells contain a copy of the chromosome. In *Escherichia coli* (*E. coli*) and other rod-shaped bacteria, the accurate partitioning process and the proper placement of the septum are precisely restricted to midcell by the effect of nucleoid occlusion [1–4] and the MinCDE protein system [1,2,5]. The nucleoid occlusion mechanism blocks Z-ring formation from all sites except the nucleoid-free-zones, while the Min system prevents the septum proteins at the cell poles [6]. The Min-protein system consists of MinC, MinD, and MinE proteins [5]. MinC is recruited to the membrane by MinD, and inhibits the formation of the septum proteins in terms of the MinCD complex [7–10]. MinE is also recruited to the membrane by MinD. In the absence of MinE, MinCD is distributed homogeneously over the entire membrane [11], which blocks septum protein formation at all sites. MinD performs oscillation pole-to-pole, driven by MinE [12]. MinC also colocalizes and cooscillates with MinD [7,8], so that the time-averaged concentration of MinC is lowest at midcell [12]. As MinC inhibits septum protein formation, the septum can assemble only near the midcell area.

According to this protein mechanism, Howard et al. [13] proposed the coarse-grained nonlinear reaction–diffusion model for studying the self-organized protein pattern and identifying midcell topological markers. Although this model is simple, it can demonstrate the oscillation pattern and positional information of the cell division process via the Min-protein system;

* Corresponding author at: R&D Group of Biological and Environmental Physics, Department of Physics, Faculty of Science, Mahidol University, Bangkok 10400, Thailand.
E-mail addresses: scwtr@mahidol.ac.th, wtriampo@gmail.com (W. Triampo).

0096-3003/$ - see front matter © 2010 Elsevier Inc. All rights reserved.
doi:10.1016/j.amc.2010.07.033

however, the dynamics is a continuum version at the macroscopic level. Recently, the mesoscopic dynamics approach assumed the implementation of the lattice Boltzmann method (LBM) [14] for the Min-protein system [15,16]. The method was shown to recover the Howard model at the macroscopic level [15,16]. In addition, the numerical results from this technique were consistent with experimental results [12,17,18]. Hence the LBM approach is an effective alternative tool for studying Min-protein oscillation, which naturally deals with particle dynamics.

LBM uses an alternative numerical scheme for simulating fluid dynamics. This method evolved from the lattice gas model, which involves many stochastic or random processes resulting in noise or fluctuations. It has provided insights into the underling particle dynamics of the physical system, whereas most other approaches focus only on the solution of the macroscopic equation. The advantage of LBM is that it is easy to implement for several shape boundaries due to the nature of particle kinetics. It is perhaps reasonable to say that LBM operates at the mesoscopic level, which is in between the microscopic (lattice gas) and macroscopic (continuum) level. Though LBM consumes tremendously large computing resources, the amount is still relatively small compared to those consumed with other approaches, like molecular dynamic and Monte Carlo simulations—which could the main reason why LBM has become the more favored method. LBM has been particularly successful in simulating fluid flow for a broad variety of complex physical systems, such as multiphase and multi-component fluids [19], advection–dispersion [20], and blood flow [21–23]. However, the LBM boundary treatments, in some situations, have critical effects on the solution at the macroscopic level. As pointed out by Zhang et al. [24], the standard boundary conditions are not accurate for the class of dispersion transport modeled by LBM. They suggested that the mirror-image method is a suitable boundary treatment to address this problem. The boundary treatment for LBM simulation is an important issue and progress is still being made [24–26].

In this present work, we re-examined the LBM boundary effects on Min-protein oscillation. We applied the impermeable boundary condition suggested by Zhang et al. and the mid-grid bounce-back boundary condition [27] to our reaction–diffusion lattice Boltzmann model. We then compared the results from two boundary conditions in both one- and two-dimensional cases. This paper is the first one to demonstrate the effect of boundary conditions in the LBM reaction diffusion model, especially on the intracellular process.

This paper is outlined as follows: In Section 2, we briefly review the reaction–diffusion model for MinCDE oscillation by Howard et al. In Section 3, the details for the LMB algorithm and boundary conditions are explained. Finally, the numerical results are discussed in Section 4.

2. Model

The dynamics of the interaction between MinD (in the complex with MinC) and MinE proteins have been proposed by Howard et al. [13] through a set of reaction–diffusion equations (RDEs). In this model, they describe the time rates of density change due to the diffusions of MinD and MinE, and the mass transfer between the cell membrane and the cytoplasm. The local mass densities for each Min-protein are denoted by: ρ_D for cytoplasmic MinD, ρ_d for membrane-bound MinD, ρ_E for cytoplasmic MinE, and ρ_e for membrane-bound MinE. In general form, the RDEs can be written as

$$\frac{\partial \rho_c}{\partial t} - D_c \frac{\partial^2 \rho_c}{\partial x_\alpha^2} = R_c, \tag{2.1}$$

where $\rho_c = \rho_c(\vec{x}, t)$ is the local mass density of protein species $c = \{D, d, E, e\}$ at position $\vec{x}$ (with x_α as the components) and time t; $R_c = R_c(\{\rho_c\})$ is the reaction term which depends on the density set of the species $\{\rho_c\}$; D_c is the isotropic diffusion coefficient. The reaction terms for each Min-protein are given by:

$$R_D = -\frac{\sigma_1 \rho_D}{1 + \sigma_1' \rho_e} + \sigma_2 \rho_e \rho_d, \tag{2.2}$$

$$R_d = \frac{\sigma_1 \rho_D}{1 + \sigma_1' \rho_e} - \sigma_2 \rho_e \rho_d, \tag{2.3}$$

$$R_E = \frac{\sigma_4 \rho_e}{1 + \sigma_4' \rho_D} - \sigma_3 \rho_D \rho_E, \tag{2.4}$$

$$R_e = -\frac{\sigma_4 \rho_e}{1 + \sigma_4' \rho_D} + \sigma_3 \rho_D \rho_E. \tag{2.5}$$

The constant σ_1 represents the association of MinD to the membrane [11]. σ_1' corresponds to the membrane-bound MinE, suppressing the recruitment of MinD from the cytoplasm. σ_2 reflects the rate that MinE on the membrane drives MinD on the membrane into the cytoplasm. Based on the evidence of the cytoplasmic interaction between MinD and MinE [28], we let σ_3 be the rate that cytoplasmic MinD recruits cytoplasmic MinE to the membrane, while σ_4 corresponds to the rate that MinE disassociates from the membrane to the cytoplasm. Finally, σ_4' corresponds to the cytoplasmic MinD, suppressing the release of the membrane-bound MinE. The time scale of the diffusion on the membrane is much slower than that in the cytoplasm. It is therefore reasonable to set D_d and D_e to zero.

In this dynamics, we allow for the Min-protein to bind/unbind from the membrane, but not for it to be degraded in the process. Thus, the total amount of each type of Min-protein is conserved. The *E. coli* cell is a close-system, therefore the appropriated boundary condition is reflecting or hard-wall. The zero-flux $J \equiv -D_c \partial \rho_c / \partial x_\alpha = 0$ is imposed at the boundary regime.

We apply the minimal linear stability analysis specifically to Min-protein RDEs [29] to determine in which conditions the oscillatory pattern is expected to generate, using the case of the one-dimensional for the sake of simplicity. For practical analysis of other RDEs systems, please refer to [30,31]. The obtained results could lead to parameter estimations, but to do this we first write our set of Eq. (2.1) in the matrix form:

$$\frac{\partial \vec{\rho}}{\partial t} = \mathbf{D}\frac{\partial^2 \vec{\rho}}{\partial x^2} + \vec{f}(\vec{\rho}), \tag{2.6}$$

where $\vec{\rho}$ is the Min-protein density vector and its elements are $\rho_c = \rho_c(x,t)$; $\mathbf{D}$ is a diagonal matrix of diffusion coefficients D_c; and $\vec{f}(\vec{\rho})$ is a vector of reaction terms R_c. By perturbing with a small variation vector $\delta\vec{\rho}$ from the homogeneous state $\vec{\rho}^*$, we can define

$$\vec{\rho} \equiv \vec{\rho}^* + \delta\vec{\rho}, \tag{2.7}$$

where $\vec{\rho}^*$ can be obtained by evaluating $\frac{\partial \vec{\rho}^*}{\partial t} = \frac{\partial \vec{\rho}^*}{\partial x_\alpha} = \vec{f}(\vec{\rho}^*) = 0$. Substituting (2.7) into (2.6) and taking a Taylor expansion to the first order, we get:

$$\frac{\partial \delta\vec{\rho}}{\partial t} = \mathbf{D}\frac{\partial^2 \delta\vec{\rho}}{\partial x^2} + \mathbf{J}^*\delta\vec{\rho}, \tag{2.8}$$

where $\mathbf{J}^* = \left.\frac{\partial \vec{f}}{\partial \vec{\rho}}\right|_{\vec{\rho}=\vec{\rho}^*}$ is the Jacobian matrix evaluated at the fix point $\vec{\rho}^*$. Applying the general solution for $\delta\vec{\rho} = \delta\vec{\rho}_0 e^{\omega t} e^{iqx}$ to Eq. (2.8), we obtain the Eigen equation

$$\mathbf{A}\delta\vec{\rho} = \omega\delta\vec{\rho}, \tag{2.9}$$

where $\mathbf{A} \equiv -\mathbf{D}q^2 + \mathbf{J}^*$, ω is the Eigen-value and q is the wave number. The real part of ω will then determine if the equation is linearly stable under a small spatial perturbation, whereas its imaginary part will determine the period of the oscillation,

$$T = \frac{2\pi}{Im(\omega)}. \tag{2.10}$$

If at least one Eigen-value ω has a real part that is positive, then the homogeneous fix point is linearly unstable under a small spatial perturbation.

Next, we apply linear stability analysis to the reaction–diffusion Eqs. (2.1)–(2.5) and obtain the matrix:

$$\mathbf{A} = \begin{bmatrix} -\frac{\sigma_1}{1+\sigma_1'\rho_e^*} - D_D q^2 & \sigma_2\rho_e^* & 0 & \frac{\sigma_1\sigma_1'\rho_D^*}{(1+\sigma_1'\rho_e^*)^2} + \sigma_2\rho_d^* \\ \frac{\sigma_1}{1+\sigma_1'\rho_e^*} & -\sigma_2\rho_e^* & 0 & -\frac{\sigma_1\sigma_1'\rho_D^*}{(1+\sigma_1'\rho_e^*)^2} - \sigma_2\rho_d^* \\ -\frac{\sigma_4\sigma_4'\rho_e^*}{(1+\sigma_4'\rho_D^*)^2} - \sigma_3\rho_E^* & 0 & -\sigma_3\rho_D^* - D_E q^2 & \frac{\sigma_4}{1+\sigma_4'\rho_D^*} \\ \frac{\sigma_4\sigma_4'\rho_e^*}{(1+\sigma_4'\rho_D^*)^2} + \sigma_3\rho_E^* & 0 & \sigma_3\rho_D^* & -\frac{\sigma_4}{1+\sigma_4'\rho_D^*} \end{bmatrix}. \tag{2.11}$$

We solve the Eigen Eq. (2.9) numerically. First, we use an iterative finite-different method to find the homogeneous fix points of our system of Eq. (2.6). We carried out the iterations several times with different starting points, using parameter values given by Howard et al. [13], and found only one fixed point, namely, $\rho_D^* = 116.873$, $\rho_E^* = 3.36183$, $\rho_d^* = 1383.13$, $\rho_e^* = 81.6382$ (in the unit of μm^{-1}). Then, with this fixed point, we are able to find the Eigen-value ω of Eq. (2.9). It was found that the positive real part of ω is maximized at $q = 1.5\ \mu m^{-1}$. This indicates the presence of a maximum linear unstable oscillating mode, with a wavelength of 4.2 μm [13,16,29].

3. Lattice Boltzmann method

The lattice Boltzmann method (LBM) for reaction–diffusion equations [32] is applied in order to simulate the Min-protein system [15,16]. The lattice Boltzmann equation (LBE) [14,27] with the Bhatnagar–Gross–Krook collision (LBGK) [33] can be written as

$$f_i^c(\vec{x} + \vec{e}_i\Delta t, t + \Delta t) - f_i^c(\vec{x}, t) = -\frac{\Delta t}{\tau_c}\left[f_i^c(\vec{x}, t) - f_i^{eq,c}(\rho_c, \vec{u})\right] + \Delta t S_i^c, \tag{3.1}$$

where $f_i^c(\vec{x}, t)$ is the single-particle distribution function of species c associated with lattice velocity $\vec{e}_i$ at position $\vec{x}$ and time t; $f_i^{eq,c}(\rho_c, \vec{u})$ is the local equilibrium corresponding Maxwellian distribution function with the local density ρ_c and local fluid speed $\vec{u}$; S_i^c is the source distribution function and τ_c is the relaxation parameter. The macroscopic quantities can be obtained from the moments of the distribution function as follows:

$$\sum_i f_i^c(\vec{x}, t) = \sum_i f_i^{eq,c}(\vec{x}, t) = \rho_c(\vec{x}, t), \tag{3.2}$$

$$\sum_i S_i^c = R_c. \tag{3.3}$$

We consider the zero mean velocity ($\vec{u} = 0$) flow. In addition, to obtain the correct reaction–diffusion equation, we need the quantities:

$$\sum_i \vec{e}_i f_i^{eq,c}(\vec{x},t) = \rho_c \vec{u} = 0, \tag{3.4}$$

$$\sum_i \vec{e}_i \vec{e}_i f_i^{eq,c}(\vec{x},t) = \sum_i e_{i,\alpha} e_{i,\beta} f_i^{eq,c}(\vec{x},t) = \rho_c c_s^2 \delta_{\alpha\beta}, \tag{3.5}$$

$$\sum_i \vec{e}_i S_i^c = 0, \tag{3.6}$$

$$\sum_i \vec{e}_i \vec{e}_i S_i^c = 0, \tag{3.7}$$

where c_s is the speed of sound. The choice of the equilibrium distribution function and the source term is dependent on the constraint in (3.2)–(3.7). We chose the equilibrium distribution

$$f_i^{eq,c} = w_i \rho_c, \tag{3.8}$$

where w_i is the lattice weight factor. For the source term, we chose the simple form

$$S_i^c = w_i R_c, \tag{3.9}$$

where R_c is macroscopic reaction as defined in (2.1), as well as in (2.2)–(2.5). The choices given in (3.8) and (3.9) are the simplest ones that can provide the correct macroscopic equations. We implement the LBM algorithm with two steps:

- *Collision step*: $\tilde{f}_i^c(\vec{x},t) = f_i^c(\vec{x},t) - \frac{\Delta t}{\tau_c}\left[f_i^c(\vec{x},t) - f_i^{eq,c}(\rho_c)\right] + \Delta t S_i^c$,
- *Streaming step*: $f_i^c(\vec{x} + \vec{e}_i \Delta t, t + \Delta t) = \tilde{f}_i^c(\vec{x},t)$.

The boundary condition is computed before streaming the resulting collision distribution function. Here we selected the impermeable boundary condition [24] and the mid-grid bounce-back boundary condition [27], which is equivalent to the hard-wall boundary at the macroscopic level. For simplicity, we set $\Delta x = \Delta t = 1$. Now let us consider the boundary domain in the 2D system for illustration, located at $\vec{b} = (x = 0, y)$. The distribution functions in this domain are not permitted to compute the collision step, but the streaming step is allowed. We define the adjacent fluid domain closest to the boundary domain located at $\vec{g} = (x = 1, y)$. If the boundary condition is mid-grid bounce-back (we will call this simply bounce-back), we calculate the unknown distribution functions as

$$f_i^c(\vec{b}) = f_i^c(\vec{b} - \vec{e}_i), \tag{3.10}$$

where $\vec{b} - \vec{e}_i \Delta t$ must be inside the fluid domain. The accuracy of this boundary condition is known as second order [27]. The impermeable boundary condition via the mirror-image method (we will call this simply mirror-image) [24] can be calculated by

$$f_i^c(\vec{b}) = f_k^c(\vec{g}), \tag{3.11}$$

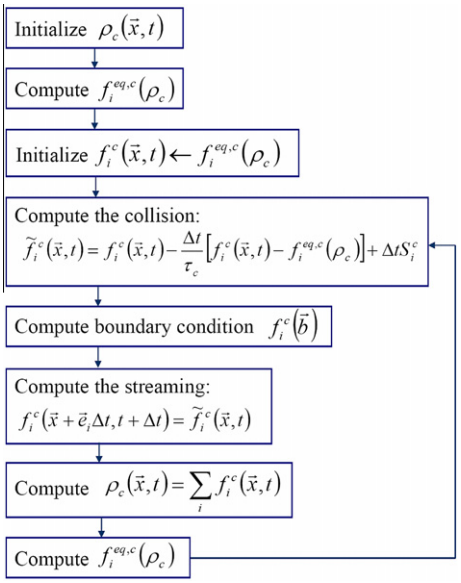

Fig. 1. The flow chart demonstrates LBM implementation.

where index k is the opposite direction of i corresponding to lattice velocity $\vec{e}_i$. The flowchart of LBM implementation is summarized in Fig. 1.

It has been shown, through the Chapman-Enskog analysis, that the continuum limit of LBE (3.1) recovers the correct reaction–diffusion equations [32]. For the D1Q3 and D2Q9 lattice model, the reaction–diffusion equation (up to the second order correction) is given by [15,16]

$$\frac{\partial \rho_c}{\partial t} - D_c \frac{\partial^2 \rho_c}{\partial x_\alpha^2} = R_c + \mathrm{O}(\partial^3), \tag{3.12}$$

where $D_c = c_s^2(\tau_c - \Delta t/2)$ is the diffusion coefficient.

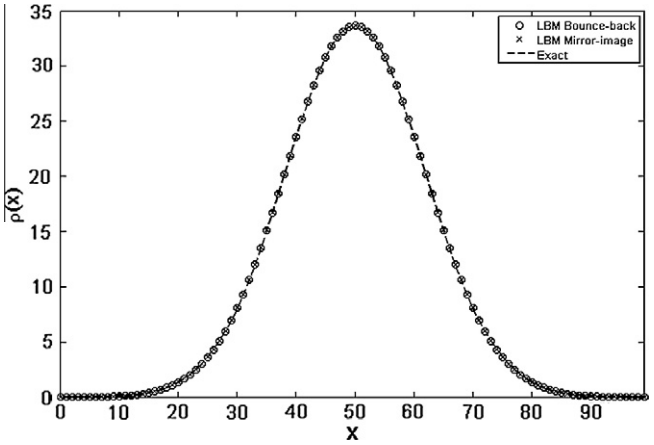

Fig. 2. The density profile $\rho(x,t)$ arrived at from LBM simulation with two different boundary conditions, bounce-back (○) and mirror-image (×), compared to the exact solution (dashed line) from Eq. (4.1). The LBM results were simulated on 100 grids with $D = 0.0028$ and data was selected at iteration 10.

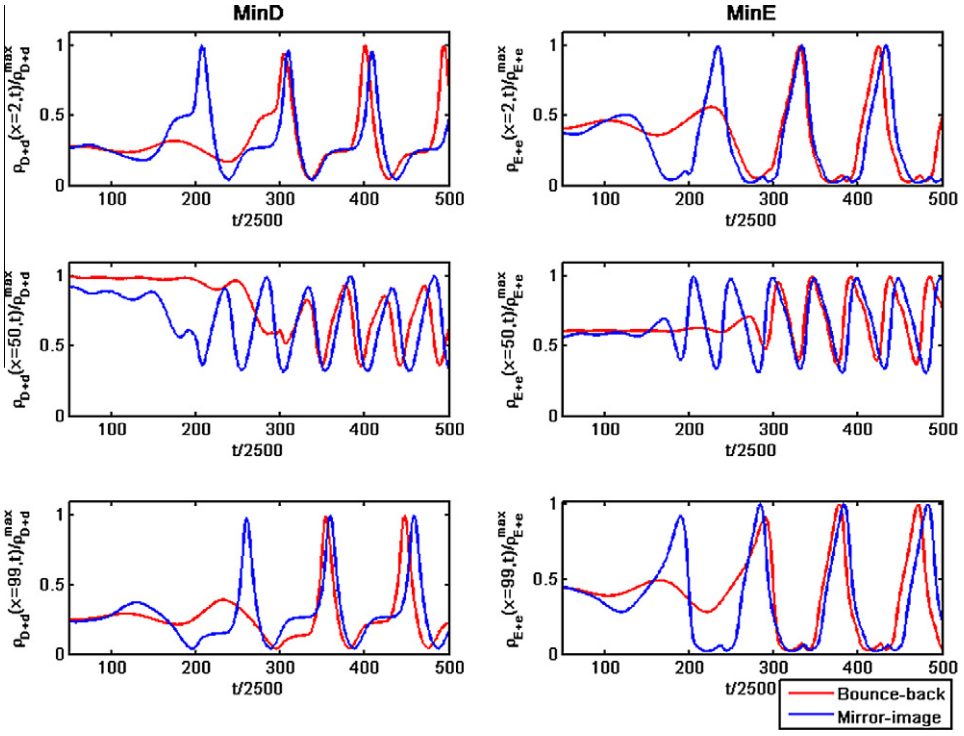

Fig. 3. The partial time evolution of normalized-densities ρ_{D+d} (left) and ρ_{E+e} (right) at the selected positions, including $x = 2$(top), $x = 99$ (bottom) and $x = 50$ (middle), for the two polar zones and middle-cell zone, respectively.

4. Numerical results and discussion

We simulated the dynamics of Min-proteins oscillation with LBM, as described in the previous section, in both one- and two-dimensional systems. For the one-dimensional system, we selected a one-dimensional lattice model with three allowed velocities (D1Q3) where the lattice velocities are defined by $\{\vec{e}_i\} = \{0, v, -v\}$, and $i = \{0,1,2\}$ is the lattice link index. The weight factors for this case are given by $w_0 = 2/3$ and $w_1 = w_2 = 1/6$. For two-dimensional system, we selected a two-dimensional square lattice model with nine allowed velocities (D2Q9) where the lattice velocities are defined by $\{\vec{e}_i\} = \{(0,0),(\pm v,0),(0,\pm v),(\pm v,\pm v)\}$, and $i = \{0,1,2,\ldots,8\}$ is the lattice link index. The weight factors for this case are given by $w_0 = 4/9$, $w_1 = w_2 = w_3 = w_4 = 1/9$ and $w_5 = w_6 = w_7 = w_8 = 1/36$. Here, $v \equiv \Delta x/\Delta t$ is the lattice speed magnitude; Δx and Δt are the lattice spacing and time step intervals, respectively. Usually, we selected $\Delta x = \Delta t = 1$, which leads to $v = 1$ (for 2D, $\Delta y = \Delta x$). Therefore our system is dimensionless. The (dimensionless) speed of sound is $c_s = \sqrt{1/3}$ for both D1Q3 and D2Q9 [34]. The relaxation time is calculated from $\tau_c = 3D_c + 0.5$ for both cases. We implemented the LBM on a PC using C programming.

First, we validated our LBM on the pure diffusion equation by dropping the reaction term (by setting $R_c = 0$) in the one-dimensional system. The system was simulated on 100 grids, which represented a bacterium 2 μm long. In this situation, we simulated only a single species of density: $\rho(x,t) \equiv \rho_c(x,t)$. The dimensionless diffusion constant was set to be $D \equiv D_c = 0.0028$. We initialized the density with a delta-like function: $\rho(x_0 = 50, t = 0) \equiv \rho_0 = 1000$. We show the density profile $\rho(x,t)$ from our LBM simulation with two different boundary conditions: bounce-back and mirror-image. We also compare these results with the exact solution:

$$\rho(x,t) = \frac{\rho_0}{\sqrt{4\pi D t}} \exp\left[-\frac{(x-x_0)^2}{4Dt}\right]. \tag{4.1}$$

The results are shown in Fig. 2.

It was seen that both numerical results from the LBM and the exact solution (4.1) are in good agreement. This indicates that the two different boundary conditions, namely bounce-back and mirror-image, have no effect whatsoever on the pure

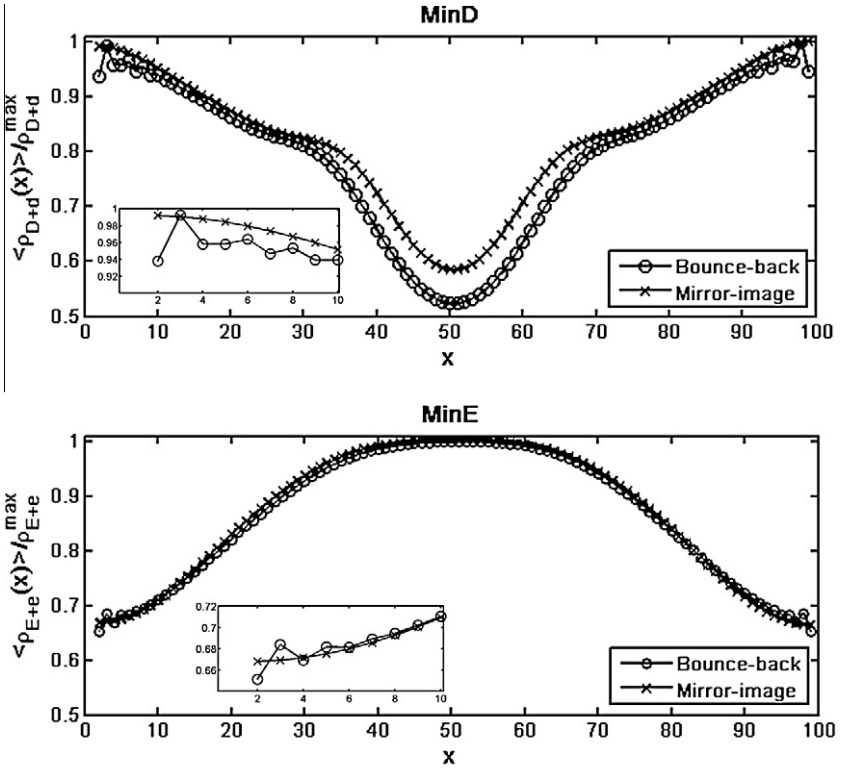

Fig. 4. The normalized-time-averaged MinD (left) and MinE (right) densities in 1D, relative to their respective time-average maxima as functions of the position along the bacterium cell, which compares the results from LBM with two different boundary conditions: bounce-back (○) and mirror-image (×). Each sub-plot magnifies as non-smooth due to the boundary effects at the polar zone.

diffusion equation. However, the boundary conditions will affect the system when we take the reaction terms into account, as we will see in the next simulation. It should be noted that since reaction terms of any given reaction–diffusion based model can greatly differ, depending on model details and dynamics, great care must be taken when making a general or universal statement about the results.

To simulate Min-protein oscillation in a one-dimensional system, we initialized the distribution function from an equilibrium state where MinD and MinE were randomly distributed as 3000 for ρ_D, 170 for ρ_E, and $\rho_d = \rho_e = 0$. We used the diffusion constants and the reaction rate parameters as used in Ref. [13], which were tested for linear stability following Section 2. However, to put them into the LBM, we need to make all parameters dimensionless. The dimensionless parameters we chose are $D_D = 0.28$, $D_E = 0.6$, $\sigma_1 = 8 \times 10^{-3}$, $\sigma_2 = 2.52 \times 10^{-2}$, $\sigma_3 = 1.6 \times 10^{-1}$, $\sigma_4 = 3.2 \times 10^{-4}$, $\sigma_1' = 280$, and $\sigma_4' = 270$. Because no diffusion occurs on the membrane, we set $D_d = D_e = 0$. We simulated the system up to 2.5×10^7 iterations. We computed the total concentration in the cytoplasm and on the membrane of each Min-protein, $\rho_{D+d} = \rho_D + \rho_d$ for MinD and $\rho_{E+e} = \rho_E + \rho_e$ for MinE, by excluding the boundary node.

The partial oscillations of Min-proteins in the one-dimensional system are shown in Fig. 3. Here, we used ρ_{D+d} and ρ_{E+e} at the selected positions, including $x = 2$, $x = 99$ (at the polar zones) and $x = 50$ (in the middle-cell zone), and then we normalized them. The (normalized) densities of Min-proteins evolve from the random-distributed initial state to the spatiotemporal oscillation state with some transient time (see Fig. 3). We noticed that the transient times of the result when using the mirror-image boundary condition are faster than when using the bounce-back boundary condition, approximately 1.5 times faster for all sets.

To observe the spatial topology of Min-proteins, we calculated the normalized-time-averaged MinD and MinE densities as functions of position, as shown in Fig. 4. The MinE normalized-averaged-density peaks at the cell middle and has a minimum at the cell rims, with MinD being nearly out of phase with MinE. This implies that MinE tries to prevent septum proteins from being formed at the cell middle site and tries to suppress the inhibitor, MinD, from this region. To validate this conclusion, we compared the numerical results to the experimental data compiled by our group members [17,18]. When we compared the LBM results with the experimental results, they were in qualitative agreement. These results are also in qualitative agreement with the experimental data by another group [12], as well as the numerical results obtained in another work [13].

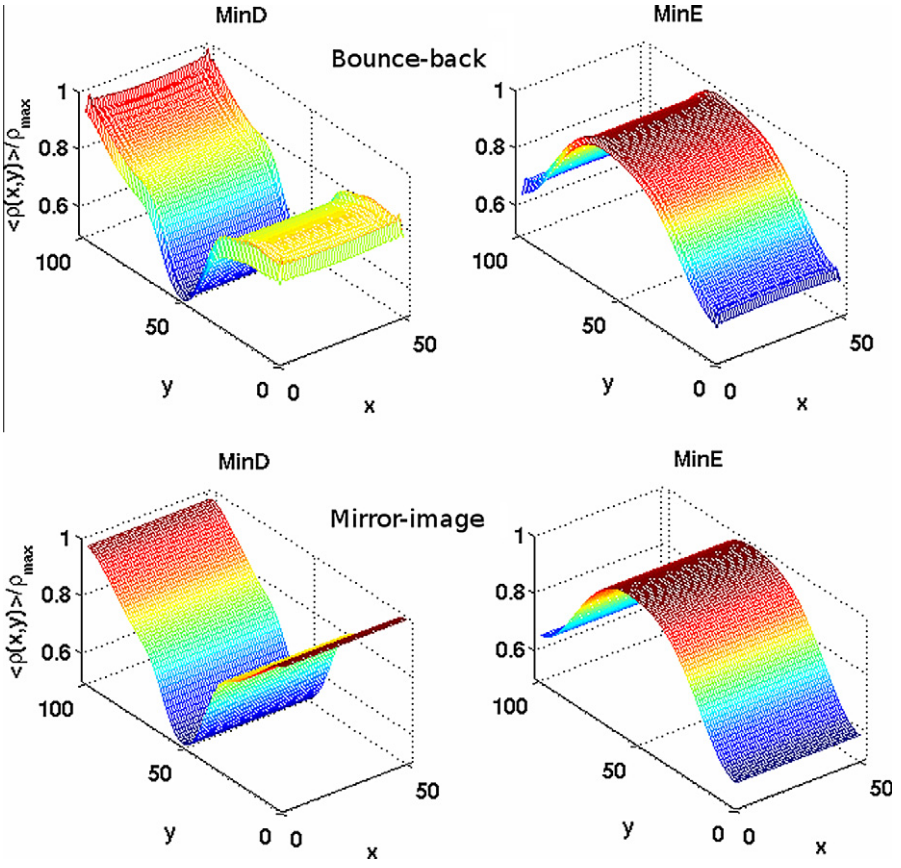

Fig. 5. The normalized-time-averaged MinD (left column) and MinE (right column) densities in 2D, relative to their respective time-average maxima as functions of the position (x,y) inside the bacterium cell. Comparison results from LBM with two different boundary conditions: bounce-back (upper row) and mirror-image (lower row).

We then extended our simulation to a two-dimensional system. The system was simulated on 50×100 grids, which represented typically a bacterium 1×2 μm in size. We initialized the distribution function from an equilibrium state where MinD and MinE were randomly distributed as 3000 for ρ_D, 170 for ρ_E, and $\rho_d = \rho_e = 0$ for each grid point. The dimensionless parameters were chosen in the same way as in the one-dimensional case. The normalized-time-averaged MinD and MinE densities as functions of position are shown in Fig. 5 for this case. It was found that the average densities of Min-proteins are nearly homogenous in x-direction; therefore the dominant dynamics oscillation of Min-proteins were expressed in y-direction. Due to this reason, the dynamics in 2D are exactly identical to that in 1D.

Regarding the effect of boundary conditions, namely bounce-back and mirror-image, on dynamic oscillation, differences in simulation results via LBM were noticeably found. We observed in the Min-protein densities at the boundary node a portion of a non-smooth curve when using the bounce-back boundary conditions, whereas the densities were found to be very smooth at the boundary node when using the mirror-image boundary condition for both one- and two-dimensional systems (see Figs. 4 and 5). This happened for both MinD and MinE, but was more prominent in the former. The difference in the degree of non-smoothness is mainly due to the difference in protein copy concentrations. Interestingly, it evidently appears that reaction terms respond differently to different boundary conditions. This may suggest that one should take greater care in boundary conditions than one might expect when applying LBM for the RDE based model, especially for the model where reactions crucially occur at the boundary.

It is worth mentioning that there are several published methods for boundary treatments via LBM for the hydrodynamics system. Among them, the bounce-back seems to be the most popular for non-slip type boundary implementation. This perhaps is due to the fact that it ensures that the components of the fluid velocity vanish at the boundary. However, this method cannot be applied to solute transport, especially the reaction–diffusion system, because the nature of dispersion-transport boundaries differs from hydrodynamics boundaries [27]. The diffusive system requires that the flux vanish ($J \equiv -D_c \partial \rho_c / \partial x_\alpha = 0$) at the boundary and the mirror-image implementation satisfies this constraint [35]. Lastly, it is obviously seen from our results that the mirror-image boundary condition is better than the bounce-back boundary condition for the simulation of this model via the LBM.

5. Concluding remarks

In this paper, we investigated the effects that boundary conditions have on the LBM when simulating the dynamic oscillation of Min-proteins and describing MinD/MinE interaction [15,16]. We applied the mirror-image boundary condition suggested by Zhang et al. and the mid-grid bounce-back boundary condition [24] to our reaction–diffusion lattice Boltzmann model. We compared the results from two boundary conditions and found that the mirror-image method is a suitable boundary condition for this Min-protein problem, as far as the smoothness of the data curves is concerned. The degree of non-smoothness varied, depending on Min-protein species or concentrations. However, more work is required to understand which boundary condition is the most appropriate for a given model. It is reasonable to say that the LBM approach could provide an alternative fast computational tool for studying Min-protein oscillation. It provides numerical results which are in qualitative agreement with experimental results [12,17,18]. However, optimization treatment, especially regarding boundary conditions, could be a very important issue. Still, we believe that the LBM is a useful scheme for simulating at the cellular level those biological systems governed by reaction–diffusion equations.

Acknowledgements

We are grateful to the anonymous reviewer for truly helpful comments. The authors thank Mr. David Blyler for reading and editing the manuscript. This work was supported by the National Center for Genetic Engineering and Biotechnology (BIOTEC), the Thailand Research Fund (TRF), the Commission on Higher Education (CHE), the Development and Promotion of Science and Technology Talents program (DPST), and the Thailand Center of Excellence in Physics.

References

[1] J. Lutkenhaus, S.G. Addinall, Bacterial cell division and the Z ring, Annu. Rev. Biochem. 66 (1997) 93–116.
[2] L. Rothfield, S. Justice, J. Garcia-Lara, Bacterial cell division, Annu. Rev. Genet. 33 (1999) 423–448.
[3] C.L. Woldringh, E. Mulder, P.G. Huls, N. Vischer, Toporegulation of bacterial division according to the nucleoid occlusion model, Res. Microbiol. 142 (1991) 309–320.
[4] X.C. Yu, W. Margolin, FtsZ ring clusters in min and partition mutants: role of both the Min system and the nucleoid in regulating FtsZ ring localization, Mol. Microbiol. 32 (1999) 315–326.
[5] P.A. de Boer, R.E. Crossley, L.I. Rothfield, A division inhibitor and a topological specificity factor coded for by the minicell locus determine proper placement of the division septum in *E. coli*, Cell 56 (1989) 641–649.
[6] K. Suefuji, R. Valluzzi, D. Ray Chaudhuri, Dynamic assembly of MinD into filament bundles modulated by ATP, phospholipids, and MinE, Proc. Natl. Acad. Sci. USA. 99 (2002) 16776–16781.
[7] P.A. de Boer, R.E. Crossley, A.R. Hand, L.I. Rothfield, The MinD protein is a membrane ATPase required for the correct placement of the *Escherichia coli* division site, EMBO J. 10 (1991) 4371–4380.
[8] D.M. Raskin, P.A. de Boer, MinDE-Dependent pole-to-pole oscillation of division inhibitor MinC in *Escherichia coli*, J. Bacteriol. 181 (1999) 6419–6424.
[9] Z. Hu, J. Lutkenhaus, Topological regulation of cell division in *Escherichia coli* involves rapid pole to pole oscillation of the division inhibitor MinC under the control of MinD and MinE, Mol. Microbiol. 34 (1999) 82–90.

[10] A.L. Marston, J. Errington, Selection of the midcell division site in *Bacillus subtilis* through MinD-dependent polar localization and activation of MinC, Mol. Microbiol. 33 (1999) 84–96.
[11] S.L. Rowland, X. Fu, M.A. Sayed, Y. Zhang, W.R. Cook, L.I. Rothfield, Membrane redistribution of the *Escherichia coli* MinD protein induced by MinE, J. Bacteriol. 182 (2000) 613–619.
[12] C.A. Hale, H. Meinhardt, P.A.J. de Boer, Dynamic localization cycle of the cell division regulator MinE in *Escherichia coli*, EMBO J. 20 (2001) 1563–1572.
[13] M. Howard, A.D. Rutenberg, S. de Vet, Dynamic compartmentalization of bacteria: accurate division in *E. coli*, Phys. Rev. Lett. 87 (2001) 278102.
[14] S. Chen, G.D. Doolen, Lattice Boltzmann method for fluid flows, Annu. Rev. Fluid Mech. 30 (1998) 329–364.
[15] W. Ngamsaad, W. Triampo, P. Kanthang, I.-M. Tang, N. Nuttawut, C. Modjung, Y. Lenbury, A lattice Boltzmann method for modeling the dynamic pole-to-pole oscillations of Min proteins for determining the position of the midcell division plane, J. Korean Phys. Soc. 46 (2005) 1025–1030.
[16] S. Sriyab, J. Yojina, W. Ngamsaad, P. Kangthang, C. Modchang, N. Nuttavut, Y. Lenbury, C. Krittanai, W. Triampo, Mesoscale modeling technique for studying the dynamics oscillation of Min protein: pattern formation analysis with lattice Boltzmann method, Comput. Biol. Med. 39 (2009) 412–424.
[17] U. Junthorn, S. Unai, P. Kangthang, W. Ngamsaad, C. Modchang, W. Triampo, C. Krittanai, D. Triampo, Y. Lenbury, Single-particle tracking method for quantitative tracking and biophysical studies of the MinE protein, J. Korean Phys. Soc. 52 (2008) 639–648.
[18] S. Unai, P. Kanthang, U. Junthon, W. Ngamsaad, W. Triampo, C. Modchang, C. Krittanai, Quantitative analysis of time-series fluorescence microscopy using a spot tracking method: application to Min protein dynamics, Biologia 64 (2009) 27–42.
[19] N.S. Martys, H.D. Chen, Simulation of multicomponent fluids in complex three-dimensional geometries by the lattice Boltzmann method, Phys. Rev. E 53 (1996) 743–750.
[20] R.G.M. van der Sman, M.H. Ernst, Advection–diffusion lattice Boltzmann scheme for irregular lattices, J. Comput. Phys. 60 (2000) 766–782.
[21] M. Hirabayashi, M. Ohta, D.A. Rufenacht, B. Chopard, A lattice Boltzmann study of blood flow in stented aneurism, FGCS 20 (2004) 925–934.
[22] C. Migliorini, Y.H. Qian, H.H. Chen, E. Brown, R. Jain, L. Munn, Red blood cells augment leukocyte rolling in a virtual blood vessel, Biophys. J. 84 (2002) 1834–1841.
[23] C.H. Sun, C. Migliorini, L. Munn, Red blood cells initiate leukocyte rolling in postcapillary expansions: a lattice Boltzmann analysis, Biophys. J. 85 (2003) 208–222.
[24] X. Zhang, J.W. Crawford, A.G. Bengough, I.M. Young, On boundary conditions in the lattice Boltzmann model for advection and anisotropic dispersion equation, Adv. Water Resour. 25 (2002) 601–609.
[25] S. Chen, D.O. Martinez, R. Mei, On boundary conditions in lattice Boltzmann methods, Phys. Fluids 8 (1996) 2527–2536.
[26] Q. Zou, X. He, On pressure and velocity boundary conditions for the lattice Boltzmann BGK model, Phys. Fluids 9 (1997) 1591–1598.
[27] S. Succi, The Lattice Boltzmann Equation: For Fluid Dynamics and Beyond, Oxford University Press, New York, 2001. p. 82.
[28] J. Huang, C. Cao, J. Lutkenhaus, Interaction between FtsZ and inhibitors of cell division, J. Bacteriol. 178 (1996) 5080–5085.
[29] C. Modchang, W. Triampo, P. Kangthang, U. Junthorn, S. Unai, W. Ngamsaad, N. Nuttavut, D. Triampo, Y. Lenbury, Stochastic modeling of external electric field effect on *Escherichia coli* Min protein dynamics, J. Korean Phys. Soc. 53 (2008) 851–862.
[30] Rui Dilão, Turing instabilities and patterns near a Hopf bifurcation, Appl. Math. Comput. 164 (2005) 391–414.
[31] V. Gafiychuk, B. Datsko, Inhomogeneous oscillatory solutions in fractional reaction–diffusion systems and their computer modeling, Appl. Math. Comput. 198 (2008) 251–260.
[32] S.P. Dawson, S. Chen, G.D. Doolen, Lattice Boltzmann computations for reaction–diffusion equations, J. Chem. Phys. 98 (1993) 514–1523.
[33] P.L. Bhatnagar, E.P. Gross, M. Krook, A model for collision processes in gases. I. Small amplitude processes in charged and neutral one-component systems, Phys. Rev. 94 (1954) 511–525.
[34] Y.H. Qian, D. d'Humieres, P.A. Lallemand, Lattice BGK models for Navier-Stokes equation, Europhys. Lett. 17 (1992) 479–484.
[35] G. Drazer, J. Koplik, Tracer dispersion in two-dimensional rough fractures, Phys. Rev. E 056104-1 (2001) 11.